

Differences in White Matter Fiber Tract Development Present From 6 to 24 Months in Infants With Autism

Jason J. Wolff, Ph.D.

Hongbin Gu, Ph.D.

Guido Gerig, Ph.D.

Jed T. Elison, Ph.D.

Martin Styner, Ph.D.

Sylvain Gouttard, M.S.

Kelly N. Botteron, M.D.

Stephen R. Dager, M.D.

Geraldine Dawson, Ph.D.

Annette M. Estes, Ph.D.

Alan C. Evans, Ph.D.

Heather C. Hazlett, Ph.D.

Penelope Kostopoulos, Ph.D.

Robert C. McKinstry, M.D., Ph.D.

Sarah J. Paterson, Ph.D.

Robert T. Schultz, Ph.D.

Lonnie Zwaigenbaum, M.D.

Joseph Piven, M.D.

For the IBIS Network

Objective: Evidence from prospective studies of high-risk infants suggests that early symptoms of autism usually emerge late in the first or early in the second year of life after a period of relatively typical development. The authors prospectively examined white matter fiber tract organization from 6 to 24 months in high-risk infants who developed autism spectrum disorders (ASDs) by 24 months.

Method: The participants were 92 high-risk infant siblings from an ongoing imaging study of autism. All participants had diffusion tensor imaging at 6 months and behavioral assessments at 24 months; a

majority contributed additional imaging data at 12 and/or 24 months. At 24 months, 28 infants met criteria for ASDs and 64 infants did not. Microstructural properties of white matter fiber tracts reported to be associated with ASDs or related behaviors were characterized by fractional anisotropy and radial and axial diffusivity.

Results: The fractional anisotropy trajectories for 12 of 15 fiber tracts differed significantly between the infants who developed ASDs and those who did not. Development for most fiber tracts in the infants with ASDs was characterized by higher fractional anisotropy values at 6 months followed by slower change over time relative to infants without ASDs. Thus, by 24 months of age, those with ASDs had lower values.

Conclusions: These results suggest that aberrant development of white matter pathways may precede the manifestation of autistic symptoms in the first year of life. Longitudinal data are critical to characterizing the dynamic age-related brain and behavior changes underlying this neurodevelopmental disorder.

(*Am J Psychiatry Wolff et al.; AiA:1-12*)

Autism spectrum disorders (ASDs) are complex disorders of neurodevelopment defined by impaired social communication and restricted, repetitive behaviors. ASDs represent a significant public health concern, affecting upward of one in 110 children, with a recurrence rate among at-risk families of nearly one in five (1, 2). Findings from prospective studies of infant siblings of children with ASDs, who are at higher than average risk for the disorder, indicate that a number of the defining behavioral features of ASDs first emerge around 12 months of age after a period of relatively typical postnatal development (3–5).

Although several studies have documented the early behavioral course of infants later diagnosed with ASDs, we know of no published neuroimaging data on such infants before toddlerhood. Existing studies have provided evidence from magnetic resonance imaging (MRI) of significantly larger than normal brain volume in 2- and 3-year olds with ASDs (6–10). These findings are consistent with

reports of higher than normal brain weight in postmortem brains of individuals with autism (11), as well as numerous reports associating ASDs with large head circumference (12). Two large retrospective studies suggest that the onset of this larger head circumference likely occurs in the latter part of the first year of life (7, 13). Taken together, findings from the behavioral studies and the studies of brain and head size growth in high-risk infant siblings suggest that the latter half of the first year of life is a pivotal time for both brain changes and symptom onset in infants later diagnosed with an ASD. The concurrent timing of these phenomena suggests that brain changes during this period may have an important role in the pathogenesis of autistic behavior.

Autism is increasingly considered a disorder characterized in part by aberrant neural circuitry (14, 15). Functional neuroimaging studies have revealed patterns of disrupted connectivity in adults (16) and children (17, 18)

with ASDs. A growing body of work has employed diffusion tensor imaging to gauge the microstructural properties of white matter circuitry (19, 20). Studies of ASDs using diffusion tensor imaging have identified evidence of widespread abnormalities in white matter fiber tract integrity (21–25), with cross-sectional studies indicating less age-related change in children and adolescents with ASDs than in typical comparison subjects (26, 27). While the preponderance of existing work suggests altered white matter development in ASDs, the extent, direction, and developmental course of these differences remain unclear (28).

Fundamentally a disorder of development, autism emerges early in life and is generally associated with life-long disability (29). When development itself is intrinsic to the phenomenon in question, it is prudent to seek answers from developmental trajectories (30–32). This is particularly so in the earliest periods of infancy, when dramatic changes in behavior are paralleled by dramatic changes in the brain. White matter pathways, for instance, rapidly develop during the first years of life, after which change is attenuated (33). However, to our knowledge, there have been no longitudinal studies of neural circuitry in ASDs, and but a few concerning volumetric brain development (8, 34, 35). Although numerous cross-sectional studies of children with ASDs posit key neurological changes relevant to the disorder, few have employed a true developmental perspective. As Karmiloff-Smith (36) aptly observed, cross-sectional neuroimaging studies of children are not tantamount to neuroimaging studies of development.

We present here a prospective, longitudinal study of white matter fiber tract development at 6, 12, and 24 months of age in infants who were at high risk for ASDs by virtue of having an older sibling with autism. In this study, we compared the subset of high-risk infants who showed evidence of ASDs by 24 months of age to those who did not. Given that both groups had a higher familial liability for ASDs than the general population, this design allowed for inferences not afforded to comparisons of high-risk children with ASDs and children at low familial risk. The focus of this study was on the development of white matter pathways selected on the basis of reported associations with ASDs or their core behavioral features (21–28).

Method

Participants

This study included data from an Autism Center of Excellence funded by the National Institutes of Health. The Infant Brain Imaging Study (IBIS), the parent network, is an ongoing study of infants at risk for autism. Four clinical data collection sites are associated with the study: University of North Carolina, Chapel Hill; University of Washington, Seattle; Children's Hospital of Philadelphia; and Washington University, St. Louis. Data were coordinated through the Montreal Neurological Institute (MNI) at McGill University, and data processing was performed at the University of North Carolina and the Scientific Computing and Imaging Institute at the University of Utah. The parent study en-

rolled and assessed 6-month-old high-risk infants who were seen for follow-up assessments at 12 and 24 months of age. Written informed consent was obtained from parents or legal guardians before enrollment, and the study procedures were approved by institutional review boards at each site.

The exclusionary criteria were 1) a significant medical condition known to affect brain development, 2) sensory impairment, 3) low birth weight (<2,200 g) or prematurity (<36 weeks gestation), 4) perinatal brain injury secondary to maternal complications or exposure to specific medications or neurotoxins (e.g., alcohol) during gestation, 5) non-English-speaking family, 6) contraindication for MRI (e.g., metal implant), 7) adoption, and 8) first-degree relative with idiopathic intellectual disability, psychosis, schizophrenia, or bipolar disorder.

The present study group included all high-risk infant siblings who received diffusion-weighted MRI scans at 6 months and for whom behavioral assessments were completed at age 24 months as of June 2011. Symptoms of ASDs were measured at 24 months by using the Autism Diagnostic Observation Schedule (37), which was completed by research-reliable administrators to maximize agreement across sites. On the basis of classifications from this scale, the high-risk infants were divided into two groups: ASD-negative (below the ASD cutoff) and ASD-positive (above the cutoff). At 24 months, 28 infants met the criteria for ASDs and 64 did not. To characterize differences in autism symptoms between groups, a severity score was generated for each participant. Symptom severity scores on the Autism Diagnostic Observation Schedule range from 1 (least severe) to 10 (most severe), with scores of 4 or higher consistent with the presence of an ASD (38). The Mullen Scales of Early Learning (39) were administered at each visit, and the early learning composite score at 24 months of age was used to characterize general cognitive ability. The composite score at 12 months was substituted in the data for four subjects who were missing complete 24-month data for the Mullen scales.

Image Acquisition

MRI brain scans were completed at the clinical sites on identical 3-T Siemens TIM Trio scanners (Siemens Medical Solutions, Malvern, Pa.) equipped with 12-channel head coils during natural sleep. The diffusion tensor imaging sequence was acquired as an *ep2d_diff* pulse sequence with a field of view of 190 mm (6 and 12 months) or 209 mm (24 months), 75–81 transversal slices, a slice thickness of 2 mm isotropic, $2 \times 2 \times 2$ -mm³ voxel resolution, a TR of 12,800–13,300 ms, a TE of 102 ms, variable b values between 0 and 1,000 s/mm², 25 gradient directions, and a scan time of 5–6 minutes. Intra- and intersite reliabilities were initially established and regularly evaluated by scanning traveling volunteers, or “phantoms,” at all sites within the same week (40).

Image Preprocessing

Data from diffusion-weighted imaging were screened by using DTIPrep software (41), which automatically detects artifacts, corrects for motion and eddy current deformations, excludes images with artifacts, and generates a full report. Expert raters manually removed scans with clear residual artifacts. Data sets with fewer than 18 (72%) gradient diffusion-weighted images after this quality procedure were excluded from further processing owing to a low signal-to-noise ratio.

Processing Pipeline

Group analysis of the data from diffusion-weighted imaging, processed by means of diffusion tensor estimates, employed an improved processing pipeline (42). This processing overcomes the major challenge in implementing tract-oriented statistics in large study groups, which is finding consistent spatial parametrization within and between groups. This includes a computational anatomy approach for nonlinear coregistration of the diffusion tensor

imaging data to a template reference coordinate frame, a process to parameterize fiber tracts to functions of length, and the mapping of individual tract geometries into common coordinates.

Computational Anatomy Mapping

Unbiased atlas building (43) was used to provide one-to-one mapping between the image data and the template atlas, wherein the atlas is built from the population of data as the centered image with the smallest deformation distances. Registration proceeds in two steps (42). The first applies linear, affine registration of diffusion-weighted imaging baseline images to a structural weighted T_2 atlas by using B-spline registration and normalized mutual information (44). This is followed by an unbiased, deformable atlas-building procedure (43) that applies large-deformation diffeomorphic metric mapping transformations. The procedure relates individual data sets to the study-specific atlas template space by means of nonlinear, invertible transformation. Tensor maps were calculated from the diffusion-weighted imaging data sets by using weighted least-squares estimation and were transformed into the atlas space with tensor reorientation by the finite strain approach (45). The transformed tensor images were averaged by using the Riemannian framework (46), resulting in a final three-dimensional average tensor atlas for tractography and tract parameterization. Longitudinal diffusion-weighted imaging data for the subjects covering ages 6 to 24 months were mapped into a common atlas space by using the preceding procedure.

Fiber Tractography

Seed label maps were created according to existing tractography methods (47, 48) and drawn in the combined atlas for regions of interest by using 3D Slicer (www.slicer.org). A secondary check of regions of interest was made by using an atlas for early childhood (33). Label maps were created for the following fiber tracts: genu, body, and splenium of the corpus callosum; fornix; inferior longitudinal fasciculus; uncinate fasciculus; anterior thalamic radiation; and anterior and posterior limbs of the internal capsule. Label maps were created bilaterally for all tracts except the corpus callosum. Fiber tracts generated in 3D Slicer were processed for spurious or incomplete streamlines by means of open source software developed in-house (FiberViewer; <http://www.ia.unc.edu/dev/>). Fractional anisotropy values were generated for each fiber tract. Fractional anisotropy is an index measuring the degree of anisotropy of local diffusivity, ranging from 0, for isotropic diffusion in fluid, to 1, for strongly directional diffusivity in highly structured axonal bundles (18, 19). Axial (λ_1) and radial $[(\lambda_2 + \lambda_3)/2]$ diffusivity values, which represent diffusion parallel and transverse to axonal directions, were also produced.

Statistical Analysis

Demographic characteristics were recorded at 6, 12, and 24 months. Potential group differences between ASD-positive and ASD-negative groups were tested for age, sex, and Mullen Scales of Early Learning composite score at each time point by using either *t* tests (age and early learning composite score) or Fisher's exact test (sex).

Longitudinal trajectories of mean fractional anisotropy values for fiber tracts in the ASD-positive and -negative groups were compared by using random coefficient linear growth curve models. The random coefficient model fits a group developmental trend while accounting for variability in individual growth trajectories. Among the 92 high-risk subjects included in the analysis, 14 subjects had data from one visit, 40 had data from two visits, and 38 had data from three visits. The mixed-model framework accommodates different patterns of missing data and unbalanced designs.

Although white matter is known to develop more rapidly in the first year of life than in the second, a linear model was deter-

mined to best fit the change in fractional anisotropy across time given the limited number of available time points. Separate random coefficient growth curve models were fit for each fiber tract with age, group, and group-by-age interaction as fixed effects and with intercept and age slope as random effects. All growth curve models included the 24-month early learning composite score as a covariate. The primary hypothesis of different age trajectories in the two groups was tested in the interaction of group and age for each tract. With parameters from the random coefficient models, we were able to estimate separate growth slopes for the ASD-positive and ASD-negative groups. Least-squares mean fractional anisotropy values were estimated for each group and contrasted at 6, 12, and 24 months to highlight differences between groups at each individual time point. For the primary analysis of fractional anisotropy trajectories, the false discovery rate was used to correct for multiple comparisons across multiple tracts. Axial and radial diffusivity were examined in a secondary analysis to fully characterize fractional anisotropy results by means of the growth model described in the preceding.

Though the sex ratios in the two groups were not significantly different, to study for potential confounding effects of sex, we ran sensitivity analyses by adding sex and sex-by-age interaction in the preceding models. The *p* values for the primary hypothesis of age-by-group interactions decreased slightly with no change to the conclusions (results not presented).

All analyses were done by means of SAS software, version 9.2 (SAS Institute, Cary, N.C.).

Results

Descriptive and demographic data are presented in Table 1. There were no differences between the ASD-negative and ASD-positive infants in age or sex ratio at the 6-, 12-, or 24-month scan ($p > 0.10$) or age at the 24-month behavioral assessment. The final Mullen early learning composite score was approximately 12 points lower in the ASD-positive group than in the ASD-negative group, as those groups were represented at each time point (6 months: $t = 2.8$, $df = 90$, $p = 0.007$; 12 months: $t = 2.5$, $df = 64$, $p = 0.01$; 24 months: $t = 2.1$, $df = 48$, $p = 0.04$). Severity scores on the Autism Diagnostic Observation Schedule at 24 months of age likewise differed significantly between groups as assessed at each time point (6 months: $t = 19.2$, $df = 90$, $p < 0.001$; 12 months: $t = 18.2$, $df = 64$, $p < 0.001$; 24 months: $t = 14.6$, $df = 48$, $p < 0.001$).

Estimates of the fractional anisotropy slope parameters with standard errors are presented for the ASD-positive and -negative groups for all tracts in Table 2. Both groups showed significant increases in fractional anisotropy from 6 to 24 months, though the rate of change for the ASD-negative group was significantly greater than that for the ASD-positive group in the bilateral limbic (fornix) and association (inferior longitudinal fasciculus and uncinate) fiber tracts. Individual and mean group trajectories for these tracts are presented in Figure 1. The changes from 6 to 24 months in fractional anisotropy for the corpus callosum subdivisions are shown in Figure 2; the change for the body was significantly different in the two groups. For projection tracts, the growth trajectories of the left anterior thalamic radiation and all internal capsule divisions were significantly steeper for the ASD-negative infants (Figure 3).

TABLE 1. Characteristics of 92 High-Risk Infants^a With and Without Evidence of Autism Spectrum Disorders (ASDs) at 24 Months of Age

Group	N	Male		Age (months)		Early Learning Composite Score on Mullen Scales of Early Learning at 24 Months ^b		Severity Score on Autism Diagnostic Observation Schedule at 24 Months	
		N	%	Mean	SD	Mean	SD	Mean	SD
Assessed at 6 months									
ASD-positive	28	21	75	6.8	0.8	90.4 ^c	23.7	6.3 ^d	1.8
ASD-negative	64	38	59	6.7	0.8	102.1	15.7	1.3	0.7
Assessed at 12 months									
ASD-positive	17	13	76	12.7	0.7	89.8 ^c	20.3	6.1 ^d	1.4
ASD-negative	49	28	57	12.7	0.6	101.3	14.5	1.3	0.6
Assessed at 24 months									
ASD-positive	17	13	76	24.5	0.6	86.6 ^c	22.0	6.0 ^d	1.6
ASD-negative	33	19	58	24.7	0.8	99.0	18.0	1.3	0.6

^a Siblings of children already diagnosed with ASDs.

^b Four subjects were missing data at 24 months, and so the score at 12 months was substituted.

^c Score for ASD-positive group significantly lower than score for ASD-negative group (two-tailed t test, $p < 0.05$).

^d Score for ASD-positive group significantly higher than score for ASD-negative group (two-tailed t test, $p < 0.001$).

TABLE 2. Linear Growth Model Estimates for Monthly Mean Change in Fractional Anisotropy of White Matter Tracts From Age 6 to 24 Months Among 92 High-Risk Infants^a With and Without Evidence of Autism Spectrum Disorders (ASDs) at 24 Months of Age

Fiber Tract and Hemisphere	Monthly Change in Fractional Anisotropy ($\times 10^{-3}$) ^b						
	ASD-Positive Group		ASD-Negative Group		Group Difference in Slope (df=1, 113) ^c		
	Slope	SE	Slope	SE	F	Raw p	Adjusted p ^d
Anterior limb of internal capsule							
Left	2.00	0.36	3.28	0.25	8.4	0.004	0.02
Right	2.28	0.36	3.23	0.25	4.8	0.03	0.04
Anterior thalamic radiation							
Left	1.12	0.33	2.07	0.23	5.6	0.03	0.03
Right	1.74	0.31	2.38	0.22	2.8	0.10	0.10
Corpus callosum							
Body	1.56	0.54	3.10	0.38	5.4	0.02	0.03
Genu	1.81	0.50	3.02	0.35	4.1	0.05	0.05
Splenium	1.33	0.70	2.94	0.49	3.6	0.06	0.07
Fornix							
Left	0.04	0.36	1.06	0.25	5.5	0.02	0.03
Right	0.01	0.34	1.16	0.24	7.8	0.006	0.02
Inferior longitudinal fasciculus							
Left	1.23	0.36	2.48	0.25	8.2	0.005	0.02
Right	1.32	0.49	2.91	0.34	7.2	0.009	0.02
Posterior limb of internal capsule							
Left	1.99	0.45	3.55	0.31	8.0	0.005	0.02
Right	1.96	0.50	3.62	0.35	7.5	0.007	0.02
Uncinate							
Left	0.75	0.35	1.89	0.24	7.1	0.009	0.02
Right	0.79	0.39	1.75	0.27	4.2	0.04	0.05

^a Siblings of children already diagnosed with ASDs. At age 12 months, N=66. At age 24 months, N=50.

^b 0=isotropic diffusion in fluid; 1=strongly directional diffusivity in highly structured axonal bundles.

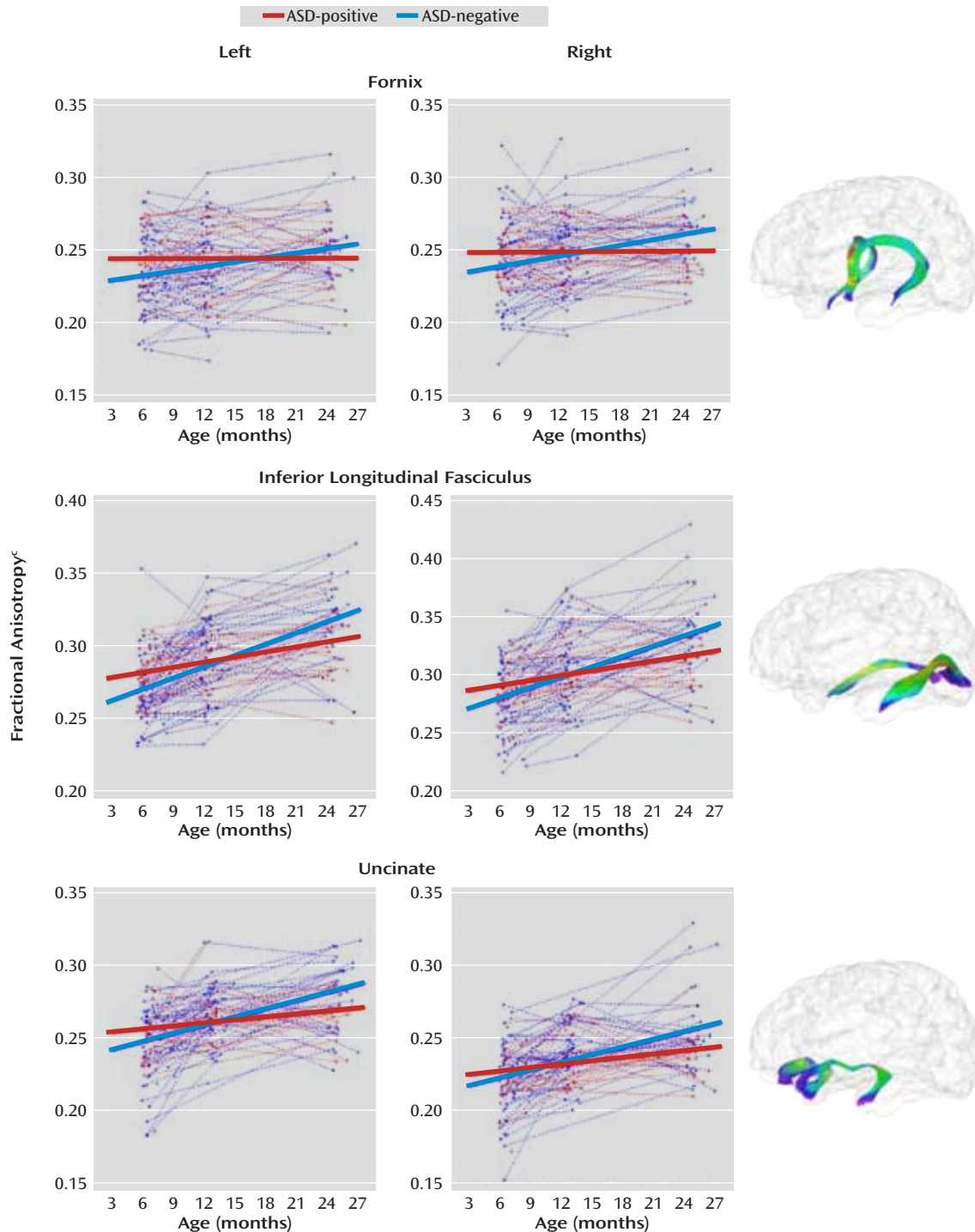
^c The group slope difference was based on the group-by-age interaction in the random coefficient growth curve model that includes intercept, Mullen Scales of Early Learning early learning composite score, age, group, and group-by-age interaction as fixed effects and intercept and age slope as random effects. The age slope and SE for each group were then estimated from the model parameters.

^d Based on the false discovery rate adjustment for multiple comparisons.

Follow-up cross-sectional analyses for mean fractional anisotropy are presented in Table 3. The mean fractional anisotropy value was significantly higher for ASD-positive than for ASD-negative infants at 6 months for the left fornix ($t=2.1$, $df=89$, $p=0.04$), left inferior longitudinal

fasciculus ($t=2.6$, $df=89$, $p=0.01$), and left uncinate ($t=2.2$, $df=89$, $p=0.03$). The mean for the body of the corpus callosum was also significantly higher in the ASD-positive infants at 6 months ($t=2.0$, $df=89$, $p=0.04$). The mean value for the right posterior limb of the internal capsule was sig-

FIGURE 1. Trajectories of Fractional Anisotropy in Limbic and Association White Matter Fiber Tracts in 92 High-Risk Infants^a With and Without Evidence of Autism Spectrum Disorders (ASDs) at 24 Months of Age^b



^a Siblings of children already diagnosed with ASDs. At age 12 months, N=66. At age 24 months, N=50.

^b Heavy lines represent mean values.

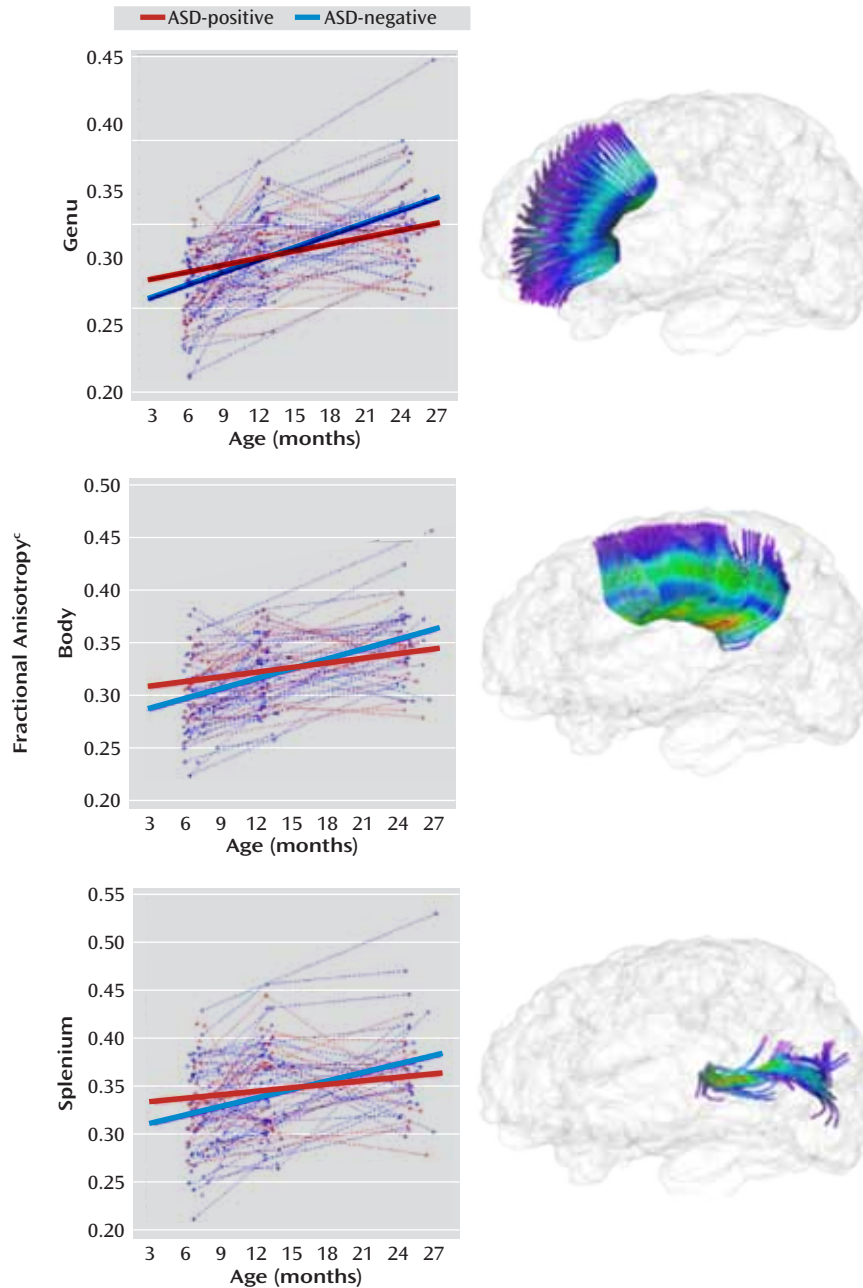
^c 0=isotropic diffusion in fluid; 1=strongly directional diffusivity in highly structured axonal bundles.

nificantly higher in the ASD-positive infants at 6 months ($t=2.1$, $df=89$, $p=0.04$), and the mean value for the left anterior limb of the internal capsule was significantly higher in the ASD-negative infants at 24 months ($t=-2.1$, $df=89$, $p=0.04$). For the left anterior thalamic radiation, the value

was significantly higher in the ASD-negative group at both 12 months ($t=-2.0$, $df=89$, $p=0.04$) and 24 months ($t=-3.0$, $df=89$, $p=0.003$).

Results from secondary analyses of axial and radial diffusivities are presented in Table 4. Linear growth trajec-

FIGURE 2. Trajectories of Fractional Anisotropy in White Matter of Corpus Callosum Subdivisions in 92 High-Risk Infants^a With and Without Evidence of Autism Spectrum Disorders (ASDs) at 24 Months of Age^b



^a Siblings of children already diagnosed with ASDs. At age 12 months, N=66. At age 24 months, N=50.

^b Heavy lines represent mean values.

^c 0=isotropic diffusion in fluid; 1=strongly directional diffusivity in highly structured axonal bundles.

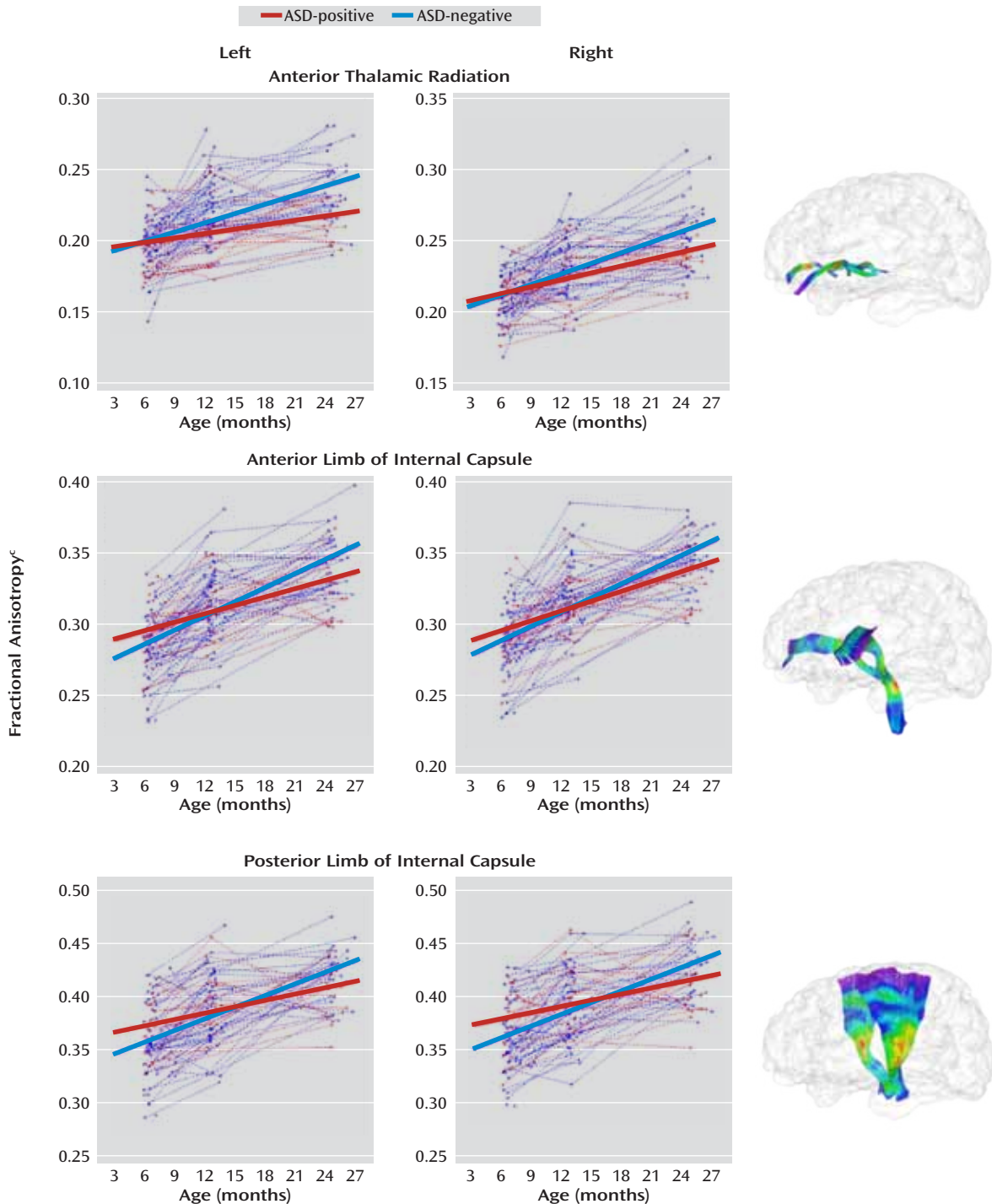
jectories did not differ significantly for these indices of tract diffusion, with the exception of the posterior limbs of the internal capsule, for which radial diffusivity was significantly higher across the 6–24-month interval for the ASD-positive group.

Discussion

These preliminary findings suggest that a distinct and pervasive course of white matter fiber tract development

characterizes high-risk infants who go on to develop autistic symptoms. Trajectories of the fractional anisotropy values for 12 of the 15 tracts examined in the present study differed significantly between groups. Most fiber tracts for the ASD-positive infants were characterized by higher fractional anisotropy at 6 months followed by blunted developmental trajectories such that fractional anisotropy was lower by 24 months. Around 12 months of age, the groups appeared similar across all tracts except the anteri-

FIGURE 3. Trajectories of Fractional Anisotropy in White Matter Projection Fiber Tracts in 92 High-Risk Infants^a With and Without Evidence of Autism Spectrum Disorders (ASDs) at 24 Months of Age^b



^a Siblings of children already diagnosed with ASDs. At age 12 months, N=66. At age 24 months, N=50.

^b Heavy lines represent mean values.

^c 0=isotropic diffusion in fluid; 1=strongly directional diffusivity in highly structured axonal bundles.

or thalamic radiation; this exception potentially indicates differential timing of development for this specific fiber bundle. Understanding why fractional anisotropy values for multiple fiber tracts are higher at 6 months but show less change over time may be critical to understanding the

development of ASDs and shed light on the neural mechanisms underlying their onset.

In agreement with findings from typically developing infants, the fractional anisotropy values for the ASD-negative infants were characterized by rapid change during the

TABLE 3. Least-Squares Mean Estimates for Difference in Group Mean Fractional Anisotropy of White Matter Tracts at Ages 6, 12, and 24 Months Between 92 High-Risk Infants^a With and Without Evidence of Autism Spectrum Disorders (ASDs) at 24 Months of Age

Fiber Tract	Difference Between ASD-Positive and -Negative Groups in Fractional Anisotropy								
	6 Months			12 Months			24 Months		
	Difference in Fractional Anisotropy ($\times 10^{-3}$) ^b			Difference in Fractional Anisotropy ($\times 10^{-3}$) ^b			Difference in Fractional Anisotropy ($\times 10^{-3}$) ^b		
	Mean	SE	t Test (p) ^c	Mean	SE	t Test (p) ^c	Mean	SE	t Test (p) ^c
Anterior limb of internal capsule									
Left	10.1	5.6	0.07	2.4	4.5	0.59	-12.9	6.3	0.04
Right	7.9	5.5	0.15	2.2	4.1	0.59	-9.1	5.5	0.10
Anterior thalamic radiation									
Left	-2.0	4.4	0.65	-7.7	3.8	0.04	-19.1	6.3	0.003
Right	1.1	3.8	0.76	-2.7	3.5	0.44	-10.4	6.2	0.10
Corpus callosum									
Body	16.3	8.0	0.04	7.1	6.5	0.28	-11.4	9.6	0.23
Genu	10.7	6.3	0.09	3.4	5.3	0.53	-11.2	9.2	0.23
Splenium	16.9	10.4	0.11	7.2	8.7	0.41	-12.2	12.7	0.34
Fornix									
Left	12.3	5.9	0.04	6.1	5.2	0.24	-6.1	7.2	0.40
Right	9.4	5.9	0.11	2.5	4.9	0.62	-11.4	6.3	0.08
Inferior longitudinal fasciculus									
Left	13.2	5.1	0.01	5.7	4.4	0.21	-9.4	4.4	0.18
Right	10.4	7.0	0.14	0.9	6.1	0.89	-18.2	9.4	0.06
Posterior limb of internal capsule									
Left	15.3	7.8	0.05	6.0	5.9	0.31	-12.7	6.7	0.06
Right	16.2	7.7	0.04	6.2	5.9	0.29	-13.7	7.9	0.08
Uncinate									
Left	10.6	4.9	0.03	3.8	3.8	0.32	-9.8	5.9	0.10
Right	5.3	5.1	0.30	-0.4	4.0	0.92	-11.9	6.4	0.07

^a Siblings of children already diagnosed with ASDs. At age 12 months, N=66. At age 24 months, N=50.

^b Value for ASD-positive group minus value for ASD-negative group. 0=isotropic diffusion in fluid; 1=strongly directional diffusivity in highly structured axonal bundles.

^c Two-tailed.

6–24-month interval (33). The blunted trajectories seen in the ASD-positive group are consistent with the lower fractional anisotropy values and comparative absence of age-related associations observed in older children and adolescents with ASDs (24, 26, 27), although these patterns may vary by fiber pathway throughout development (25, 28). The differences between the high-risk groups in this study are particularly striking considering evidence that individuals with ASDs and nonaffected family members of individuals with ASDs share a neural phenotype consisting of specific structural and functional brain abnormalities (49, 50). In a follow-up analysis, we examined axial and radial diffusivity measures to elucidate the fractional anisotropy results. With a few exceptions, the trajectories for these diffusivity measures did not significantly differ between groups, suggesting that the fractional anisotropy results stem in part from the proportional relationship of axial and radial diffusivity and not from one measure alone.

The altered trajectories of development seen here ostensibly begin in advance of the onset of clinical symptoms (3–5), suggesting that core behavioral features of ASDs may arise from an altered neurobiological foundation. In-

stantiated by these preliminary results, the organization of neural networks underlying ASDs appears to be characterized by atypical patterns of connectivity that differ across systems and time (14–17) and are not specific to any single brain region or behavioral domain. The relevance of developmental trajectories to understanding these dynamic processes is undeniable (30–32). Had the present study included only cross-sectional data centered at 12 months, for instance, it might have followed that the anterior thalamic radiation is uniquely relevant to the early development of ASDs. The wider view afforded by longitudinal data indicates that thalamic afferents are but one of many tracts implicated in the disorder, with associations at 12 months likely resulting from differential development.

Both highly experience-dependent and less environmentally mediated processes contribute to the functional and structural organization of the brain, and the dynamic interplay of these processes over time yields specialized cortical circuits designed to optimally process complex information (51). For example, differences in structural organization prior to a period of experience-dependent development related to social cognition (52–54) may decrease

TABLE 4. Linear Growth Model Estimates for Monthly Mean Change in Axial and Radial Diffusivity of White Matter Fiber Tracts in 92 High-Risk Infants^a With and Without Evidence of Autism Spectrum Disorders (ASDs) at 24 Months of Age

Fiber Tract	Axial Diffusivity					Radial Diffusivity				
	Mean Monthly Change (mm ² /s × 10 ⁻⁶)				F Test (p) ^b	Mean Monthly Change (mm ² /s × 10 ⁻⁶)				F Test (p) ^b
	ASD-Positive Group		ASD-Negative Group			ASD-Positive Group		ASD-Negative Group		
Slope	SE	Slope	SE	Slope	SE	Slope	SE	Slope	SE	
Anterior limb of internal capsule										
Left	2.3	1.7	2.6	1.2	0.87	-1.2	1.2	-3.0	0.0	0.23
Right	-0.7	1.3	1.1	0.0	0.25	-3.7	0.0	-3.5	0.0	0.89
Anterior thalamic radiation										
Left	-6.5	0.0	-5.8	0.0	0.46	-6.4	0.0	-7.0	0.0	0.41
Right	-6.2	0.0	-5.2	0.0	0.25	-6.6	0.0	-7.1	0.0	0.52
Corpus callosum										
Body	-10.0	1.3	-9.4	0.0	0.69	-8.2	0.0	-9.9	0.0	0.07
Genu	-10.0	1.2	-8.1	0.0	0.11	-9.1	0.0	-9.1	0.0	0.98
Splenium	-5.1	0.0	-4.8	0.0	0.85	-5.2	0.0	-7.2	0.0	0.09
Fornix										
Left	-7.2	4.0	-10.0	2.8	0.37	-6.0	2.6	-10.0	1.8	0.13
Right	-4.3	3.2	-7.2	4.0	0.92	-2.9	2.6	-5.4	1.4	0.33
Inferior longitudinal fasciculus										
Left	-10.0	1.6	-8.5	1.1	0.19	-8.2	0.0	-8.8	0.0	0.53
Right	-7.7	1.3	-6.2	0.0	0.36	-6.7	0.0	-7.9	0.0	0.18
Posterior limb of internal capsule										
Left	-3.6	0.0	-4.4	0.0	0.40	-4.5	0.0	-7.4	0.0	0.004
Right	-2.6	0.0	-3.6	0.0	0.28	-3.9	0.0	-6.9	0.0	0.003
Uncinate										
Left	-6.5	0.0	-5.9	0.0	0.61	-5.4	0.0	-6.6	0.0	0.19
Right	-6.0	0.0	-5.3	0.0	0.44	-5.2	0.0	-6.1	0.0	0.29

^a Siblings of children already diagnosed with ASDs. At age 12 months, N=66. At age 24 months, N=50.

^b Two-tailed, df=1, 113.

neural plasticity through limitations on environmental input, preventing typical neural specialization (52). These alterations could have a ripple effect through decreasing environmental responsiveness and escalating invariance, thus canalizing a specific neural trajectory that results in the behavioral phenotype that defines ASDs. In typical development, the selective refinement of neural connections through axonal pruning (55) along with constructive processes such as myelination (56) combine to yield efficient signal transmission among brain regions. One or both of these mechanisms may underlie the widespread differences in white matter fiber pathways observed in the current study. Although diffusion tensor imaging indirectly measures axonal organization, the present findings may reflect connective properties secondary to atypical activity-dependent neuronal modulation and development resulting from disordered molecular mechanisms (57). It is intriguing that our data are consistent with recent evidence from postmortem stereological research (58) and mouse models of autism (59) suggesting that axonal plasticity may be implicated in the development of ASDs.

It is clear that the neurodevelopmental story of ASDs neither begins at 6 months of age nor ends at 24. Extending neuroimaging downward to infants younger than 6 months would help clarify the temporal origin of diverging

trajectories, while extending neuroimaging to later ages would capture increasingly stable neurobehavioral outcomes. Additional data points would likewise refine the calibration of trajectories beyond linear models. Because the present results are limited to at-risk infants, the inclusion of a low-risk comparison group is necessary to frame group trajectories in the context of typical development. The addition of a multimodal approach to neuroimaging could sharpen our understanding of early brain changes in ASDs, allowing for the investigation of functional and structural covariance. Linking the structural integrity of specific fiber tracts to behaviors relevant to autism during infancy would similarly clarify mutually dependent developmental processes. To capture the mechanisms that engender and maintain the trajectories evidenced here, future researchers might also consider the role of genetic and epigenetic variables in the development of structural neural circuitry. For instance, *CNTNAP2*, which has been associated with ASDs (60), is necessary to neuron-glia interactions and may mediate axonal development by way of activity-dependent oligodendrocyte functioning (56).

Finally, the presence of significant differences in fractional anisotropy at 6 months raises the exciting possibility of developing imaging biomarkers for risk of ASDs in advance of symptom onset. Future work might investigate

the potential of predictive models for ASDs in early infancy, a process that could include refined imaging techniques or combined biobehavioral markers. Identifying infants at highest risk for ASDs before the full syndrome is manifest offers the possibility of implementing interventions that could reduce or even prevent the manifestation of the full syndrome (61).

There are several limitations to the present study. The absence of a low-risk contrast group limits interpretation of the results outside of a familial background for ASDs. It is possible, for example, that trajectories for the ASD-negative group reflect developmental resilience to or compensation for neuropathology related to familial risk. Although fractional anisotropy corresponds to organizational properties indicative of development (19, 33) as well as histological findings (62), it is an imperfect index of white matter microstructure and may reflect the effects of axonal packing, crossing fibers, or partial volumes related to noise in the data from diffusion tensor imaging (20, 63). In this study, ASD status was based on Autism Diagnostic Observation Schedule scores at 24 months. Follow-up assessment at 36–48 months of age would provide greater assurance of diagnostic outcomes.

To our knowledge, this longitudinal study has identified the earliest brain differences related to later symptoms of autism to date. The aberrant development of multiple white matter pathways seen here, along with previously reported brain and behavioral change during infancy (3–9), suggests a period of critical importance to the pathogenesis of ASDs. A developmental approach to brain and behavioral changes during this time, sensitive to characterizing longitudinal trajectories, is crucial to understanding the complexities inherent to the neurodevelopmental processes implicated in the emergence of ASDs.

Acknowledgments

The Infant Brain Imaging Study (IBIS) Network clinical sites are located at the University of North Carolina (J. Piven, IBIS Network primary investigator; H.C. Hazlett, C. Chappell); the University of Washington (S.R. Dager, A.M. Estes, D. Shaw); Washington University (K.N. Botteron, R.C. McKinstry, J. Constantino, J. Pruett); Children's Hospital of Philadelphia (R.T. Schultz, S.J. Paterson); and the University of Alberta (L. Zwaigenbaum). The data coordinating center is at the Montreal Neurological Institute (A.C. Evans, D.L. Collins, G.B. Pike, P. Kostopoulos, S. Das). The image processing core is at the University of Utah (G. Gerig) and the University of North Carolina (M. Styner). The statistical analysis core is at the University of North Carolina (H. Gu). The genetics analysis core is at the University of North Carolina (P. Sullivan, F. Wright).

Received Sept. 28, 2011; revision received Nov. 12, 2011; accepted Dec. 5, 2011 (doi: 10.1176/appi.ajp.2011.11091447). From the Carolina Institute for Developmental Disabilities and the Department of Psychiatry, University of North Carolina, Chapel Hill; the Scientific Computing and Imaging Institute, University of Utah, Salt Lake City; the Department of Psychiatry and the Department of Radiology, Mallinckrodt Institute of Radiology, Washington University School of Medicine, St. Louis; the Department of Radiology and the Department of Speech and Hearing Sciences, University of Washington, Seattle; Autism Speaks, New York; Montreal Neurological Institute, Mc-

Gill University, Montreal; the Center for Autism Research, Children's Hospital of Philadelphia, and the University of Pennsylvania, Philadelphia; and the Department of Pediatrics, University of Alberta, Edmonton. Address correspondence to Dr. Wolff (jason.wolff@cidd.unc.edu).

Dr. Evans reports having a 20% equity position in Biospective, Inc., an imaging contract research organization, as founder, and receiving a consulting fee from Biospective. All other authors report no financial relationships with commercial interests.

Supported by grants from the National Institute of Child Health and Development (HD-055741, HD-055741-S1, HD-03110, HD-40127), Autism Speaks, and the Simons Foundation. Further support was provided by the National Alliance for Medical Image Computing, funded by the National Institute of Biomedical Imaging and Bioengineering through grant EB-005149.

The authors thank the IBIS children and their families for their participation; Varun Puvanesarajah and Eric Maltbie for assisting with tractography; and Rachel G. Smith, Cheryl Dietrich, and Mahshid Farzinfar for the DWI/DTI correction and quality control efforts.

References

1. Kogan MD, Blumberg SJ, Schieve LA, Boyle CA, Perrin JM, Ghandour RM, Singh GK, Strickland BB, Trevathan E, van Dyck PC: Prevalence of parent-reported diagnosis of autism spectrum disorder among children in the US, 2007. *Pediatrics* 2009; 124:1396–1403
2. Ozonoff S, Young G, Carter A, Messinger D, Yirmiya N, Zwaigenbaum L, Bryson S, Carver LJ, Constantino JN, Dobkins K, Hutman T, Iverson JM, Landa R, Rogers SJ, Sigman M, Stone WL: Recurrence risk for autism spectrum disorders: a Baby Siblings Research Consortium study. *Pediatrics* 2011; 128:e488–e495
3. Landa R, Garret-Mayer E: Development in infants with autism spectrum disorders: a prospective study. *J Child Psychol Psychiatry* 2006; 47:629–638
4. Ozonoff S, Iosi A, Baguio F, Cook IC, Hill MM, Hutman T, Rogers SJ, Rozga A, Sangha S, Sigman MB, Young GS: A prospective study of the emergence of early behavioral signs of autism. *J Am Acad Child Adolesc Psychiatry* 2010; 49:256–266
5. Zwaigenbaum L, Bryson S, Rogers T, Roberts W, Brian J, Szatmari P: Behavioral manifestations of autism in the first year of life. *Int J Neurosci* 2005; 23:143–152
6. Courchesne E, Karns C, Davis HR, Ziccardi RA, Carper ZD, Tigue HJ, Chisum P, Moses K, Pierce K, Lord C, Lincoln AJ, Pizzo S, Schreibman L, Haas RH, Akshoomoff NA, Courchesne RY: Unusual brain growth patterns in early life in patients with autistic disorder: an MRI study. *Neurology* 2001; 57:245–254
7. Hazlett HC, Poe M, Gerig G, Smith RG, Provenzale J, Ross A, Gilmore J, Piven J: Magnetic resonance imaging and head circumference study of brain size in autism: birth through age 2 years. *Arch Gen Psychiatry* 2005; 6:1366–1376
8. Hazlett HC, Poe M, Gerig G, Styner M, Chappell C, Smith RG, Vachet C, Piven J: Early brain overgrowth in autism associated with an increase in cortical surface area before age 2 years. *Arch Gen Psychiatry* 2011; 68:467–476
9. Schumann CM, Bloss CS, Barnes CC, Wideman GM, Carper RA, Akshoomoff N, Pierce K, Hagler D, Schork N, Lord C, Courchesne E: Longitudinal magnetic resonance imaging study of cortical development through early childhood in autism. *J Neurosci* 2010; 30:4419–4427
10. Sparks BF, Friedman SD, Shaw DW, Aylward EH, Echelard D, Artru AA, Maravilla KR, Giedd JN, Munson J, Dawson G, Dager SR: Brain structural abnormalities in young children with autism spectrum disorder. *Neurology* 2002; 59:184–192
11. Bailey A, Luthert P, Dean A, Harding B, Janota I, Montgomery M, Rutter M, Lantos P: A clinicopathological study of autism. *Brain* 1998; 121:889–905
12. Lainhart JE, Piven J, Wzorek M, Landa R, Santangelo SL, Coon H,

- Folstein SE: Macrocephaly in children and adults with autism. *J Am Acad Child Adolesc Psychiatry* 1997; 36:282–290
13. Constantino JN, Majumdar P, Bottini A, Arvin M, Virkud Y, Simons P, Spitznagel E: Infant head growth in male siblings of children with and without autism spectrum disorders. *J Neurodev Disord* 2010; 2:39–46
 14. Belmonte MK, Allen G, Beckel-Mitchener A, Boulanger LM, Carper RA, Webb SJ: Autism and abnormal development of brain connectivity. *J Neurosci* 2004; 24:9228–9231
 15. Minshew NJ, Williams DL: The new neurobiology of autism: cortex, connectivity, and neuronal organization. *Arch Neurol* 2007; 64:945–950
 16. Just MA, Cherkassky VL, Keller TA, Minshew NJ: Cortical activation and synchronization during sentence comprehension in high-functioning autism: evidence of underconnectivity. *Brain* 2004; 127:1811–1821
 17. Di Martino A, Kelly C, Grzadzinski R, Zuo XN, Mennes M, Mairena MA, Lord C, Castellanos FX, Milham MP: Aberrant striatal functional connectivity in children with autism. *Biol Psychiatry* 2011; 69:847–856
 18. Dinstein I, Pierce K, Eylar L, Solso S, Malach R, Behrmann M, Courchesne E: Disrupted neural synchronization in toddlers with autism. *Neuron* 2011; 70:1218–1225
 19. Hüppi PS, Dubois J: Diffusion tensor imaging of brain development. *Semin Fetal Neonatal Med* 2006; 11:489–497
 20. Mori S, Zhang J: Principles of diffusion tensor imaging and its applications to basic neuroscience research. *Neuron* 2006; 51:527–539
 21. Alexander AL, Lee JE, Lazar M, Boudos R, DuBray MB, Oakes TR, Miller JN, Lu J, Jeong EK, McMahon WM, Bigler ED, Lainhart JE: Diffusion tensor imaging of the corpus callosum in autism. *Neuroimage* 2007; 34:61–73
 22. Barnea-Goraly N, Lotspeich LJ, Reiss AL: Similar white matter aberrations in children with autism and their unaffected siblings. *Arch Gen Psychiatry* 2010; 67:1052–1060
 23. Cheon K, Kim Y, Ohio S, Park S, Yoon H, Herrington J, Nair A, Koh Y, Jang D, Kim Y, Leventhal BL, Cho Z, Castellanos FX, Schultz RT: Involvement of the anterior thalamic radiation in boys with high functioning autism spectrum disorders: a diffusion tensor imaging study. *Brain Res* 2011; 1417:77–86
 24. Jou RJ, Jackowski AP, Papademetris X, Rajeevan N, Staib LH, Volkmar FR: Diffusion tensor imaging in autism spectrum disorders: preliminary evidence of abnormal neural connectivity. *Aust NZ J Psychiatry* 2011; 45:153–162
 25. Keller TA, Kana RK, Just MA: A developmental study of the structural integrity of white matter in autism. *Neuroreport* 2007; 18:23–27
 26. Cheng Y, Chou KH, Chen IY, Fan YT, Decety J, Lin CP: Atypical development of white matter microstructure in adolescents with autism spectrum disorders. *Neuroimage* 2010; 50:873–882
 27. Shukla DK, Keehn B, Müller R: Tract-specific analyses of diffusion tensor imaging show widespread white matter compromise in autism spectrum disorder. *J Child Psychol Psychiatry* 2011; 52:285–296
 28. Weinstein M, Ben-Sira L, Levy Y, Zachor DA, Ben Itzhak E, Artzi M, Tarrasch R, Eksteine PM, Hendler T, Ben Bashat D: Abnormal white matter integrity in young children with autism. *Hum Brain Mapp* 2011; 32:534–543
 29. Howlin P, Goode S, Hutton J, Rutter M: Adult outcome for children with autism. *J Child Psychol Psychiatry* 2004; 45:212–229
 30. Giedd JN, Blumenthal J, Jeffries NO, Castellanos FX, Liu H, Zijdenbos A, Paus T, Evans AC, Rapoport JL: Brain development during childhood and adolescence: a longitudinal MRI study. *Nat Neurosci* 1999; 2:861–863
 31. Karmiloff-Smith A: Development itself is the key to understanding developmental disorders. *Trends Cogn Sci* 1998; 2:389–398
 32. Shaw P, Greenstein D, Lerch J, Clasen L, Lenroot R, Gogtay N, Evans A, Rapoport J, Giedd J: Intellectual ability and cortical development in children and adolescents. *Nature* 2006; 440:676–679
 33. Hermoye L, Saint-Martin C, Cosnard G, Lee S, Kim J, Nassogne MC, Menten R, Clapuyt P, Donohue PK, Hua K, Wakana S, Jiang H, van Zijl PC, Mori S: Pediatric diffusion tensor imaging: normal database and observation of the white matter maturation in early childhood. *Neuroimage* 2006; 29:493–504
 34. Courchesne E, Campbell K, Solso S: Brain growth across the life span in autism: age-specific changes in anatomical pathology. *Brain Res* 2011; 1380:138–145
 35. Hardan AY, Libove RA, Keshavan MS, Melhem NM, Minshew NJ: A preliminary longitudinal magnetic resonance imaging study of brain volume and cortical thickness in autism. *Biol Psychiatry* 2009; 66:320–326
 36. Karmiloff-Smith A: Neuroimaging of the developing brain: taking “developing” seriously. *Hum Brain Mapp* 2010; 31:934–941
 37. Lord C, Rutter M, DiLavore PC, Risi S: Autism Diagnostic Observation Schedule. Los Angeles, Calif, Western Psychological Services, 2000
 38. Gotham K, Pickles A, Lord C: Standardizing ADOS scores for a measure of severity in autism spectrum disorders. *J Autism Dev Disord* 2009; 39:693–705
 39. Mullen EM: Mullen Scales of Early Learning: AGS Edition. Circle Pines, Minn, AGS Publishing, 1995
 40. Gouttard S, Styner M, Prastawa M, Gerig G: Assessment of reliability of multi-site neuroimaging via traveling phantom study. *Med Image Comput Assist Interv* 2008; 11(pt 2):263–270
 41. Liu Z, Wang Y, Gerig G, Gouttard S, Tao R, Fletcher T, Styner MA: Quality control of diffusion weighted images. *Proc SPIE* 2010; 7628:76280J
 42. Goodlett CB, Fletcher PT, Gilmore JH, Gerig G: Group analysis of DTI fiber tract statistics with application to neurodevelopment. *Neuroimage* 2009; 45(1 suppl):S133–S142
 43. Joshi S, Davis B, Jomier M, Gerig G: Unbiased diffeomorphic atlas construction for computational anatomy. *Neuroimage* 2004; 23(suppl 1):S151–S160
 44. Rueckert D, Sonoda LI, Hayes C, Hill DLG, Leach MO, Hawkes DJ: Non-rigid registration using free-form deformations: application to breast MR images. *IEEE Trans Med Imaging* 1999; 18:712–721
 45. Alexander D, Pierpaoli C, Basser PJ, Gee J: Spatial transformations of diffusion tensor magnetic resonance images. *IEEE Trans Med Imaging* 2001; 20:1131–1140
 46. Fletcher PT, Joshi S: Riemannian geometry for the statistical analysis of diffusion tensor data. *Signal Processing* 2007; 87:250–262
 47. Catani M, Thiebaut de Schotten M: A diffusion tensor imaging tractography atlas for virtual in vivo dissections. *Cortex* 2008; 44:1105–1132
 48. Mori S, Wakana S, Nagae-Poetscher LM, van Zijl PCM: MRI Atlas of Human White Matter. Amsterdam, Elsevier, 2005
 49. Kaiser MD, Hudac CM, Shultz S, Lee SM, Cheung C, Berken AM, Deen B, Pitskel NB, Sugrue DR, Voos AC, Saulnier CA, Ventola P, Wolf JM, Klin A, Vander Wyk BC, Pelphrey KA: Neural signatures of autism. *Proc Natl Acad Sci USA* 2010; 107:21223–21228
 50. Lainhart JE, Bigler ED, Bocian M, Coon H, Dinh E, Dawson G, Deutsch CK, Dunn M, Estes A, Tager-Flusterberg H, Folstein S, Hepburn S, Hyman S, McMahon W, Minshew N, Munson J, Osann K, Ozonoff S, Rodier P, Rogers S, Sigman M, Spence MA, Stodgell CJ, Volkmar F: Head circumference and height in autism: a study by the Collaborative Program of Excellence in Autism. *Am J Med Genet* 2006; 140:2257–2274
 51. Johnson MH: Interactive specialization: a domain-general framework for human functional brain development? *Dev Cogn Neurosci* 2011; 1:7–21
 52. Blasi A, Mercure E, Lloyd-Fox S, Thomson A, Brammer M, Sau-

- ter D, Deeley Q, Barker GJ, Renvall V, Deoni S, Gasston D, Williams SC, Johnson MH, Simmons A, Murphy DG: Early specialization for voice and emotion processing in the infant brain. *Curr Biol* 2011; 21:1220–1224
53. Carpenter M, Nagell K, Tomasello M: Social cognition, joint attention, and communicative competence from 9 to 15 months of age. *Monogr Soc Res Child Dev* 1998; 63:1–143
 54. Kuhl PK, Tsao FM, Liu HM: Foreign-language experience in infancy: effects of short-term exposure and social interaction on phonetic learning. *Proc Natl Acad Sci USA* 2003; 100:9096–9101
 55. Luo L, O’Leary DD: Axon regeneration and degeneration in development and disease. *Annu Rev Neurosci* 2005; 28:127–156
 56. Wake H, Lee PR, Fields RD: Control of local protein synthesis and initial events of myelination by action potentials. *Science* 2011; 333:1647–1651
 57. Zoghbi HY: Postnatal neurodevelopmental disorders: meeting at the synapse? *Science* 2003; 302:826–830
 58. Zikopoulos B, Barbas H: Changes in prefrontal axons may disrupt the network in autism. *J Neurosci* 2011; 30:14595–14609
 59. Testa-Silva G, Loebel A, Giugliano M, de Kock CP, Mansvelder HD, Meredith RM: Hyperconnectivity and slow synapses during early development of medial prefrontal cortex in a mouse model for mental retardation and autism. *Cereb Cortex* (Epub ahead of print, Aug 19, 2011)
 60. Scott-Van Zeeland AA, Abrahams BS, Alvarez-Reuerto AI, Sonnenblick LI, Rudie JD, Ghahremani D, Mumford JA, Poldrack RA, Dapretto M, Geschwind DH, Bookheimer SY: Altered functional connectivity in frontal lobe circuits is associated with variation in the autism risk gene *CNTNAP2*. *Sci Transl Med* 2010; 2:56–80
 61. Dawson G: Early behavioral intervention, brain plasticity, and the prevention of autism spectrum disorder. *Dev Psychopathol* 2008; 20:775–803
 62. Concha L, Livy DJ, Beaulieu C, Wheatley BM, Gross DW: In vivo diffusion tensor imaging and histopathology of the fimbria-fornix in temporal lobe epilepsy. *J Neurosci* 2010; 30:996–1002
 63. Mori S, van Zijl PCM: Fiber tracking: principles and strategies—a technical review. *NMR Biomed* 2002; 15:468–480